Optics Letters

The quantum Gaussian–Schell model: a link between classical and quantum optics

Riley B. Dawkins, Mingyuan Hong, Chenglong You,* and Omar S. Magaña-Loaiza

Quantum Photonics Laboratory, Department of Physics & Astronomy, Louisiana State University, Baton Rouge, Louisiana, 70803, USA
**cyou2@lsu.edu*

Received 30 January 2024; revised 27 June 2024; accepted 9 July 2024; posted 10 July 2024; published 22 July 2024

The quantum theory of the electromagnetic field uncovered that classical forms of light were indeed produced by distinct superpositions of nonclassical multiphoton wave packets. This situation prevails for partially coherent light, the most common kind of classical light. Here, for the first time, to our knowledge, we demonstrate the extraction of the constituent multiphoton quantum systems of a partially coherent light field. We shift from the realm of classical optics to the domain of quantum optics via a quantum representation of partially coherent light using its complex-Gaussian statistical properties. Our formulation of the quantum Gaussian–Schell model (GSM) unveils the possibility of performing photon-number-resolving (PNR) detection to isolate the constituent quantum multiphoton wave packets of a classical light field. We experimentally verified the coherence properties of isolated vacuum systems and wave packets with up to 16 photons. Our findings not only demonstrate the possibility of observing quantum properties of classical macroscopic objects but also establish a fundamental bridge between the classical and quantum worlds.

https://doi.org/10.1364/OL.520444

The work performed by Allan Schell in 1961 shaped the field of optical physics and specifically the classical theory of optical coherence [1,2]. His approach to describe spatial coherence of classical light fields laid the foundations for the development of optical technology ranging from imaging instruments and spectroscopy to communication [3–7]. This model, now known as the Gaussian–Schell model (GSM), enables describing classical coherence of optical wavefronts with different polarization and spectral properties [4,6–11]. Interestingly, this model also enables modeling of propagating light in complex media [5,12,13]. In addition, these ideas have been extended to nano-optical systems to describe photonic fields scattered by sub-wavelength nanostructures [14–18]. Even though the GSM originates from the classical theory of electromagnetic radiation, its versatility has enabled describing classical degrees of freedom of quantum optical systems [6,19,20]. Specific examples include the modeling of the polarization, spectral, and orbital angular momentum properties of single and entangled photons [6,19–22].

While the GSM fails to capture the intrinsic quantum properties of light, the quantum theory of electromagnetic radiation developed by Glauber and Sudarshan provides an elegant description for the excitation mode of the optical field [22–24]. Further, it provides the formalism to describe the quantum statistical properties of the light field and its quantum properties of coherence [25–27]. Indeed, these fundamental properties of photons are widely used to classify diverse kinds of light such as sunlight, laser radiation, and molecule fluorescence [25,28]. Notably, the most common type of light, classified under the umbrella of partially coherent light, can also be described using the classical theory of optical coherence [2,8]. As such, partially coherent light beams are typically categorized as classical macroscopic optical systems [29–31]. Indeed, there has been interest in investigating the boundary between classical and quantum physics through the coherence properties of partially coherent optical beams [32–34]. However, no previous studies have attempted to explore the constituent quantum multiphoton subsystems of classical partially coherent light.

Here, we establish a direct link between classical and quantum optics through the formulation of the quantum Gaussian–Schell (QGS) model. Remarkably, this model unveils the possibility of extracting the quantum multiphoton subsystems that constitute a classical partially coherent light field [23,24,31]. For the first time, we use photon-number-resolving (PNR) detection to experimentally isolate the vacuum dynamics of a partially coherent light beam [27,35]. Furthermore, we discuss the quantum coherence properties of multiphoton wave packets extracted from a classical light beam. We report experimental results for wave packets with up to 16 photons. The QGS model makes use of the complex-Gaussian statistical fluctuations inherent to partially coherent light [36–38]. Indeed, our model explains how the quantum statistical fluctuations of the electromagnetic field give rise to the formation of macroscopic spatial correlations of partially coherent light. Surprisingly, we find that the quantum dynamics of the extracted multiphoton systems can be contrary to those of the classical system hosting them. This effect demonstrates the lack of a direct correspondence between the classical and quantum worlds [39]. Thus, we believe that the QGS model will have dramatic implications for quantum technologies [40–43].

As depicted in Fig. 1, we are interested in describing the quantum properties of coherence of the multiphoton systems that form partially coherent light. For the sake of generality, we consider a partially coherent light field produced by a rotating ground glass [44,45]. This partially coherent field can be modeled through the indistinguishable superposition of coherent

and thermal light beams. The coherent component results from the unaffected beam transmitted by the ground glass, whereas the thermal contribution is produced by many diffusers on the rotating ground glass that scatter the laser beam into many independent wave packets [44,45]. The collective properties of the resulting classical beam can be described by the following cross-spectral density function (see Supplement 1):

$$W(s_1,s_2) = \langle E^{(-)}(s_1)E^{(+)}(s_2)\rangle = \mu^*(s_1)\mu(s_2) + \sqrt{\bar{n}(s_1)\bar{n}(s_2)}\,g(s_1-s_2), \tag{1}$$

for transverse-spatial positions s_1 and s_2. Here, $\mu(s_i)$ denotes the average electric field amplitude $\langle E^{(+)}(s_i)\rangle$ at point s_i, $\bar{n}(s_i) \propto \mathrm{Exp}\left[-|s_i|^2/\sigma_0\right]$ represents the mean photon number at point s_i, and $g(s_1-s_2) \propto \mathrm{Exp}\left[-|s_1-s_2|^2/\sigma_1\right]$ is the normalized correlation term between the two points, where σ_0 and σ_1 are real, positive constants. The ensemble average $\langle\cdot\rangle$ is calculated with respect to the complex random variables $E^{(+)}(s_i)$, representing the electric field [8,46]. As discussed below, the inherent complex-Gaussian statistics of this beam enable the precise determination of its quantum statistics. To obtain the density matrix of the beam, we must first determine the probability density function for $E^{(+)}(s_1)$ and $E^{(+)}(s_2)$. This approach enables us to express the ensemble average $\langle\cdot\rangle$ in the form of an integral, incorporating the statistical characteristics of the electric field. The benefit of this method is the ability to compute expectation values for more complex structures than simple finite-degree polynomials of the electric field. For simplicity, we denote $E^{(+)}(s_1) \equiv \alpha$, $E^{(+)}(s_2) \equiv \beta$, $\mu(s_i) \equiv \mu_i$, $\bar{n}(s_i) \equiv \bar{n}_i$, and $g(s_1-s_2) \equiv g$.

Notably, we capture the quantum statistical properties of our field through the probability density of a real-Gaussian random

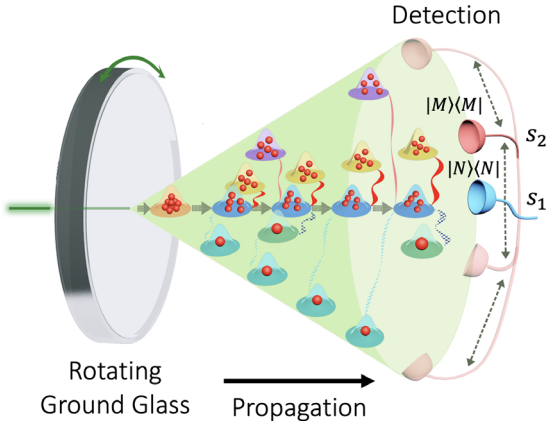

Fig. 1. Multiphoton wave packet dynamics of partially coherent light. This diagram illustrates the generation of a partially coherent light field from a rotating ground glass [44]. The macroscopic classical system is formed by many scattered multiphoton wave packets exhibiting distinct quantum dynamics [45]. For example, we illustrate bunching between five-photon wave packets (red, solid) and anti-bunching between five- and one-photon wave packets (blue, dotted). We isolate these multiphoton systems by performing projective measurements using photon-number-resolving detection [27,35]. In our experiment, we use two detectors, one of which is fixed at the center of the detection plane, whereas the other is scanned through the wavefront of the scattered field. We conclude our experiment by performing multiphoton correlations between the two detectors. The outcomes of this experiment are described by the quantum Gaussian–Schell model.

four-vector $\boldsymbol{r}$ [47]. Here, the corresponding probability density is

$$P(\boldsymbol{r}) = \frac{1}{4\pi^2\sqrt{|\boldsymbol{\Gamma}|}}\, e^{-\frac{1}{2}(\boldsymbol{r}-\boldsymbol{\mu})^T\boldsymbol{\Gamma}^{-1}(\boldsymbol{r}-\boldsymbol{\mu})}, \tag{2}$$

where $\boldsymbol{\mu} = \langle\boldsymbol{r}\rangle$ is the mean of $\boldsymbol{r} = (\mathrm{Re}[\alpha], \mathrm{Im}[\alpha], \mathrm{Re}[\beta], \mathrm{Im}[\beta])$, $\Gamma_{ij} = \langle r_i r_j\rangle - \langle r_i\rangle\langle r_j\rangle$ is the covariance matrix of $\boldsymbol{r}$, and $|\cdot|$ represents the determinant. The critical aspect of Eq. (2) is its exponent, where the correlations between random variables are manifested as products between them. Specifically, we calculate the mean vector as $\boldsymbol{\mu} = (\mathrm{Re}[\mu_1], \mathrm{Im}[\mu_1], \mathrm{Re}[\mu_2], \mathrm{Im}[\mu_2])$ and the covariance matrix between the two positions as

$$\boldsymbol{\Gamma} = \frac{1}{2}\begin{pmatrix} \bar{n}_1 & 0 & g\sqrt{\bar{n}_1\bar{n}_2} & 0 \\ 0 & \bar{n}_1 & 0 & g\sqrt{\bar{n}_1\bar{n}_2} \\ g\sqrt{\bar{n}_1\bar{n}_2} & 0 & \bar{n}_2 & 0 \\ 0 & g\sqrt{\bar{n}_1\bar{n}_2} & 0 & \bar{n}_2 \end{pmatrix}. \tag{3}$$

Using Eq. (2) and our expressions for $\boldsymbol{\mu}$ and $\boldsymbol{\Gamma}$, we can express the statistics of partially coherent light through its probability density function over coherent amplitudes α and β:

$$P(\alpha,\beta) = \frac{1}{\pi^2\bar{n}_1\bar{n}_2(1-g^2)}\mathrm{Exp}\left[-\frac{|\alpha-\mu_1|^2}{\bar{n}_1(1-g^2)} - \frac{|\beta-\mu_2|^2}{\bar{n}_2(1-g^2)} + 2g\frac{\mathrm{Re}\left[(\alpha-\mu_1)^*(\beta-\mu_2)\right]}{\sqrt{\bar{n}_1\bar{n}_2}(1-g^2)}\right]. \tag{4}$$

The amplitudes α and β are centered around their respective means, with spatial coherence properties described by g. As a result, in the limit where $g \to 1$, the covariance matrix becomes degenerate (i.e., $|\boldsymbol{\Gamma}| \to 0$), and the probability density function will instead become a probability distribution. Finally, when s_1 and s_2 are significantly different ($g \to 0$), the correlation term vanishes, resulting in two separate Gaussian distributions.

Remarkably, transitioning from the classical to the quantum description of our optical beam is now a straightforward process. This is because each instance of $E^{(+)}(s_i)$ in the classical ensemble corresponds to a coherent excitation [48]. Thus, the density matrix of our beam, in terms of the excitation basis, can be written as

$$\hat{\rho}^D_{QGS} = \int d^2\alpha d^2\beta \frac{1}{\pi^2(\bar{n}_1+\tilde{n}_1)^2(1-g^2)} \times \mathrm{Exp}\left[-\frac{|\alpha-\tilde{\mu}_1|^2+|\beta-\tilde{\mu}_2|^2}{(\bar{n}_1+\bar{n}_2)(1+g)} - g\frac{|\alpha-\beta+\tilde{\mu}_2-\tilde{\mu}_1|^2}{(1-g^2)(\bar{n}_1+\bar{n}_2)}\right] \times |\alpha c_\theta, \beta s_\theta\rangle\langle\alpha c_\theta, \beta s_\theta|, \tag{5}$$

where $c_\theta \equiv \cos(\theta) = \sqrt{\bar{n}_1/(\bar{n}_1+\bar{n}_2)}$, $s_\theta \equiv \sin(\theta) = \sqrt{\bar{n}_2/(\bar{n}_1+\bar{n}_2)}$, $\tilde{\mu}_1 = \mu_1 c_\theta^{-1}$, and $\tilde{\mu}_2 = \mu_2 s_\theta^{-1}$. Note that the two modes refer to two spatially separate detectors. Additionally, the superscript D stands for "detector perspective," which indicates that the information about the detectors' configuration is entirely contained in the density matrix $\hat{\rho}^D_{QGS}$ (see Supplement 1). It is worth noticing that Eq. (5) provides a suitable description to model the projection of a classical macroscopic light beam into its constituent multiphoton wave packets. These projections are experimentally implemented using photon-number-resolving detection [27,35]. Further, Eq. (5) enables describing the spatial correlation properties of isolated multiphoton subsystems. Interestingly, when $\mu_1 = \mu_2 = 0$, our beam reduces to the well-known GSM beam, which is characterized by photon statistics that always follow a thermal distribution [8,48].

The above description of a QGS model source, while useful for understanding stationary instances of our beam, does not contain enough information to determine its evolution. This will require knowledge of our beam's underlying mode structure. Fortunately, we can utilize Eq. (5), together with the spatial mode structure of our light beam, to write its total quantum state as a functional integral (see Supplement 1):

$$\hat{\rho}^{S}_{QGS} = \int d\Sigma \, |\alpha_0\rangle\langle\alpha_0|_{\Sigma}. \tag{6}$$

Here, S stands for "state perspective," indicating that the information about the detectors' configuration is entirely contained in the detection operators and that the density matrix $\hat{\rho}^{S}_{QGS}$ only contains information about the beam itself. We further note that $|\alpha_0\rangle_{\Sigma}$ is a coherent state characterized by a coherent amplitude α_0 and a mode structure given by $\hat{a} = \int ds \Sigma(s)\hat{a}(s)$. Additionally, the functional integral is over the random mode structure $\Sigma(s)$. Thus, we can use the following rule:

$$\int d\Sigma \, f(\mathbf{\Sigma}) = \int d\mathbf{\Sigma} \, P(\mathbf{\Sigma}) f(\mathbf{\Sigma}), \tag{7}$$

where $\mathbf{\Sigma} \equiv \left(\mathrm{Re}[\Sigma(s_1)], \mathrm{Im}[\Sigma(s_1)], \ldots, \mathrm{Re}[\Sigma(s_n)], \mathrm{Im}[\Sigma(s_n)]\right)$ is a finite-dimensional vector of length $2n$, $f(\mathbf{\Sigma})$ is a function of the $\Sigma(s_i)$, and $P(\mathbf{\Sigma})$ is Eq. (2) adapted to the variables present in $\mathbf{\Sigma}$. One can show that the statistical behavior of Eq. (6) is identical to that of Eq. (5), given appropriate choices of α_0, $\boldsymbol{\mu}$ and $\mathbf{\Gamma}$. Moreover, Eq. (6) has the additional benefit of a mode structure, which is necessary in determining the state's dynamical evolution through optical systems. Now, while the realization of the QGS model given by Eq. (6) often proves to be more beneficial, Eq. (5) remains valuable for its simplicity and as an important link between the classical GSM and the QGS model. Indeed, without the representation given in Eq. (5), we would lack the basis on which to claim that Eq. (6) represents the unique quantization of a partially coherent beam.

Now, we are in a position to explore how the underlying distribution of multiphoton wave packets in the QGS model gives rise to the macroscopic properties of coherence in Eq. (1). To do this, we compute the correlation properties between multiphoton wave packets at the spatial locations s_1 and s_2. We can rewrite Eq. (5) in the Fock state basis as $\hat{\rho}^{D}_{QGS} = \sum_{n,m,k,l=0}^{\infty} p_{\mathrm{nmkl}} |n,m\rangle\langle k,l|$, which allows us to define a multiphoton wave packet correlation function $\tilde{g}^{(2)}(N,M)$ as follows (see Supplement 1 for explicit computation):

$$\tilde{g}^{(2)}(N,M) = \frac{p_{\mathrm{NMNM}}}{\left(\sum_{m=0}^{\infty} p_{\mathrm{NmNm}}\right)\left(\sum_{n=0}^{\infty} p_{\mathrm{nMnM}}\right)}. \tag{8}$$

Here, $p_{\mathrm{NMKL}} = \mathrm{Tr}\left[\hat{\rho}^{D}_{QGS}\hat{n}_{\mathrm{NMKL}}\right]$ is the probability associated with the Fock-projection operator $|N,M\rangle\langle K,L|$. Given that the probability of observing a specific multiphoton wave packet is proportional to its number of occurrences, $\tilde{g}^{(2)}(N,M)$ effectively becomes the standard coherence function [22]. Specifically, $\tilde{g}^{(2)}(N,M)$ characterizes the coherence of N-photon wave packets at the s_1-detector with M-photon wave packets at the s_2-detector. Thus, the coherence function $\tilde{g}^{(2)}(N,M)$ is crucial for demonstrating the underlying nonclassical multiphoton coherence in partially coherent light sources, which can be critical for various applications in quantum information sciences [14–19,28,41,42,49].

We now verify the nonclassical properties of coherence of the constituent multiphoton subsystems of a partially coherent light field. Our technique for generating partially coherent light is depicted in Fig. 1 (see Supplement 1 for additional details). Specifically, we experimentally generate a partially coherent light beam with a degree of second-order coherence $g^{(2)}(0)$ of 1.70 ± 0.01. This beam is passed through a beam splitter that produces two light fields that are measured by two PNR detectors [21]. The first detector remains fixed at the center of the beam, whereas the second detector is moved along a transverse spatial axis. We report the correlation measurements for various choices of multiphoton wave packets in Fig. 2. While the trace of the classical partially coherent beam shows bunching properties, its constituent quantum multiphoton subsystems can exhibit very different dynamics. Surprisingly, the spatially separated multiphoton subsystems with a vastly different number of particles exhibit antibunching, which is produced by the quantum nature of the light field [22,50]. However, the spatially separated multiphoton subsystems with a similar number of particles show bunching effects like the classical hosting system. Interestingly, a similar behavior is observed for the correlation of the vacuum-fluctuation component of the field. Notably, the quantum Gaussian–Schell model introduced in this Letter captures all the complex multiphoton dynamics hosted by partially coherent light. Furthermore, these results demonstrate that there is not a direct correspondence between the coherence properties of the classical partially coherent light field and its constituent multiphoton wave packets [39]. In addition, these measurements

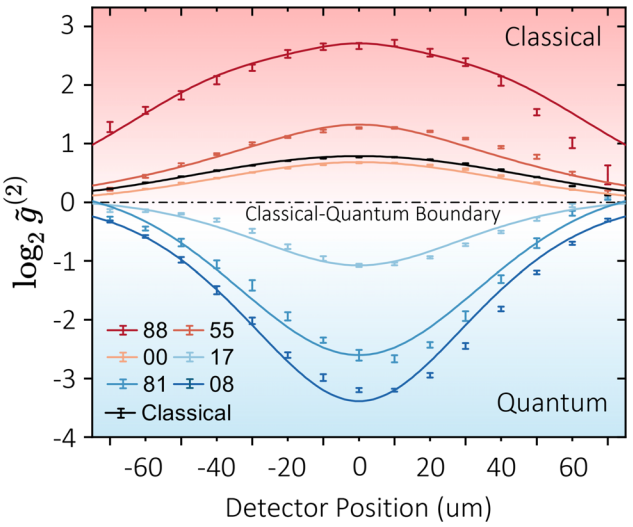

Fig. 2. Classical and quantum coherence of multiphoton wave packets. We present the experimental results of the process depicted in Fig. 1. Specifically, one detector was fixed at the center of the source, and the position of the second is given on the horizontal axis. On the vertical axis, we plot $\log_2 \tilde{g}^{(2)}(N,M)$ for some of the constituent multiphoton wave packets of the partially coherent light beam. We present these results for various choices of N, M ranging from subsystems with 0–16 photons. Additionally, the classical $\log_2 g^{(2)}$ for the partially coherent light beam is shown in black. The theoretical fitting of this data was accomplished using Eq. (8), which describes the coherence properties of the extracted multiphoton subsystems. Interestingly, wave packets whose $\tilde{g}^{(2)}$ have a positive logarithm exhibit classical properties of coherence, while those with a negative logarithm of $\tilde{g}^{(2)}$ show quantum coherence properties. This kind of multiphoton subsystems cannot be described through the classical formulation of the Gaussian–Schell model [4–18].

show the possibility of extracting quantum multiphoton systems from classical light fields.

It is also worth mentioning the potential applications of the QGS model in studying multiple scattered light [51]. Specifically, there has been much interest in the effects of random propagation through complex media on quantum sources [52,53]. We believe that the field-theoretic average over coherent states given in Eqs. (6) and (7) could provide an avenue for studying the effects of partial coherence on more complicated quantum systems. This approach has potential to greatly simplify our understanding of these effects and has greater implications for nanophotonics [43] and quantum imaging [54], given the scattering is sufficiently random that complex-Gaussian statistics are valid.

Our demonstration of the quantum Gaussian–Schell model establishes a direct relationship between the classical and quantum worlds [29–34]. This is achieved by extracting the constituent multiphoton quantum subsystems of a classical partially coherent light field. As a result of our predictions, we have for the first time experimentally isolated the vacuum and multiphoton dynamics of this kind of light field by implementing photon-number-resolving detection [27,35]. Our theory unveils surprising quantum coherence properties of multiphoton wave packets, which have been observed in subsystems with up to 16 photons. This uncovers the possibility of observing quantum properties within macroscopic classical objects. Furthermore, the quantum Gaussian–Schell model, leveraging complex-Gaussian statistical properties, elucidates the formation of macroscopic spatial correlations in partially coherent light [36–38]. It also reveals surprising differences between the quantum dynamics of the constituent multiphoton wave packets and their hosting classical system. Consequently, we believe that our work has profound implications for quantum imaging [19,28,41], quantum nanophotonics [14–18,49], and the preparation of multiparticle systems for quantum information science [16,41,42].

Funding. National Science Foundation (CPS-2312086).

Acknowledgment. We acknowledge funding from the National Science Foundation through Grant No. CPS-2312086. We thank Dr. Ivan Agullo and Dr. Roberto de J. León-Montiel for their very useful discussions.

Disclosures. The authors declare no conflicts of interest.

Data availability. Data underlying the results presented in this Letter are not publicly available at this time but may be obtained from the authors upon reasonable request.

Supplemental document. See Supplement 1 for supporting content.

REFERENCES

1. A. C. Schell, "The multiple plate antenna," Ph.D. thesis, Massachusetts Institute of Technology (1961).
2. M. Born and E. Wolf, *Principles of Optics: Electromagnetic Theory of Propagation, Interference and Diffraction of Light*, 7th ed. (Cambridge University Press, Cambridge, 1999).
3. R. Zhang, N. Hu, H. Zhou, *et al.*, Nat. Photonics **15**, 743 (2021).
4. R. Dutta, M. Korhonen, A. T. Friberg, *et al.*, J. Opt. Soc. Am. A **31**, 637 (2014).
5. D. J. Wheeler and J. D. Schmidt, J. Opt. Soc. Am. A **28**, 1224 (2011).
6. L. Chen, Light: Sci. Appl. **10**, 148 (2021).
7. Y. Liu, X. Zhang, Z. Dong, *et al.*, Phys. Rev. Appl. **17**, 024043 (2022).
8. E. Wolf, *Introduction to the Theory of Coherence and Polarization of Light* (Cambridge University Press, 2007).
9. X. Peng, L. Liu, F. Wang, *et al.*, Opt. Express **26**, 33956 (2018).
10. C. Yan, X. Li, Y. Cai, *et al.*, Phys. Rev. A **106**, 063522 (2022).
11. B. Rodenburg, M. Mirhosseini, O. S. Maga na-Loaiza, *et al.*, J. Opt. Soc. Am. B **31**, A51 (2014).
12. G. P. Agrawal and E. Wolf, J. Opt. Soc. Am. A **17**, 2019 (2000).
13. T. Shirai, A. Dogariu, and E. Wolf, J. Opt. Soc. Am. A **20**, 1094 (2003).
14. J. Yu, Y. Xu, S. Lin, *et al.*, Phys. Rev. A **106**, 033511 (2022).
15. G. Gbur and E. Wolf, Opt. Commun. **199**, 295 (2001).
16. C. You, A. C. Nellikka, I. D. Leon, *et al.*, Nanophotonics **9**, 1243 (2020).
17. J. M. Auñón, F. J. Valdivia-Valero, and M. Nieto-Vesperinas, J. Opt. Soc. Am. A **31**, 206 (2014).
18. L. Liu, W. Liu, F. Wang, *et al.*, Nano Lett. **22**, 6342 (2022).
19. G. Nirala, S. T. Pradyumna, A. Kumar, *et al.*, Sci. Adv. **9**, eadf9161 (2023).
20. L. Hutter, G. Lima, and S. P. Walborn, Phys. Rev. Lett. **125**, 193602 (2020).
21. C. You, A. Miller, R. d. J. León-Montiel, *et al.*, npj Quantum Inf **9**, 50 (2023).
22. L. Mandel and E. Wolf, *Optical Coherence and Quantum Optics* (Cambridge University Press, 1995).
23. R. J. Glauber, Phys. Rev. **131**, 2766 (1963).
24. E. C. G. Sudarshan, Phys. Rev. Lett. **10**, 277 (1963).
25. O. S. Maga na-Loaiza, R. de J. León-Montiel, A. Perez-Leija, *et al.*, npj Quantum Inf **5**, 80 (2019).
26. C. You, M. Hong, N. Bhusal, *et al.*, Nat. Commun. **12**, 5161 (2021).
27. C. You, M. A. Quiroz-Juárez, A. Lambert, *et al.*, Appl. Phys. Rev. **7**, 021404 (2020).
28. N. Bhusal, M. Hong, A. Miller, *et al.*, npj Quantum Inf **8**, 83 (2022).
29. K. Modi, A. Brodutch, H. Cable, *et al.*, Rev. Mod. Phys. **84**, 1655 (2012).
30. W. H. Zurek, Phys. Today **44**, 36 (1991).
31. F. Fröwis, P. Sekatski, W. Dür, *et al.*, Rev. Mod. Phys. **90**, 025004 (2018).
32. F. De Martini and F. Sciarrino, Rev. Mod. Phys. **84**, 1765 (2012).
33. X.-F. Qian, B. Little, J. C. Howell, *et al.*, Optica **2**, 611 (2015).
34. X.-F. Qian, A. N. Vamivakas, and J. H. Eberly, Opt. Photonics News **28**, 34 (2017).
35. C. You, M. Hong, P. Bierhorst, *et al.*, Appl. Phys. Rev. **8**, 041406 (2021).
36. R. H. Brown and R. Q. Twiss, Nature **177**, 27 (1956).
37. O. S. Magaña-Loaiza, M. Mirhosseini, R. M. Cross, *et al.*, Sci. Adv. **2**, e1501143 (2016).
38. Y. Bromberg, Y. Lahini, E. Small, *et al.*, Nat. Photonics **4**, 721 (2010).
39. G. Jaeger, Am. J. Phys. **82**, 896 (2014).
40. A. E. Willner, H. Huang, Y. Ya, *et al.*, Adv. Opt. Photonics **7**, 66 (2015).
41. O. S. Magaña-Loaiza and R. W. Boyd, Rep. Prog. Phys. **82**, 124401 (2019).
42. F. Dell'Anno, S. De Siena, and F. Illuminati, Phys. Rep. **428**, 53 (2006).
43. M. Hong, R. B. Dawkins, B. Bertoni, *et al.*, Nat. Phys. **20**, 830 (2024).
44. F. T. Arecchi, Phys. Rev. Lett. **15**, 912 (1965).
45. T. A. Smith and Y. Shih, Phys. Rev. Lett. **120**, 063606 (2018).
46. O. Korotkova, *Random Light Beams: Theory and Applications* (CRC Press, 2017).
47. S. J. Prince, *Computer Vision: Models, Learning, and Inference* (Cambridge University Press, 2012).
48. Z. J. Ou, *Quantum Optics for Experimentalists* (World Scientific Publishing Company, 2017).
49. M. S. Tame, K. R. McEnery, Ş. K. Özdemir, *et al.*, Nat. Phys. **9**, 329 (2013).
50. W. A. T. Nogueira, S. P. Walborn, S. Pádua, *et al.*, Phys. Rev. Lett. **86**, 4009 (2001).
51. C.-C. Cheng and M. G. Raymer, Phys. Rev. A **62**, 023811 (2000).
52. S. Smolka, O. L. Muskens, A. Lagendijk, *et al.*, Phys. Rev. A **83**, 043819 (2011).
53. P. Lodahl, A. P. Mosk, and A. Lagendijk, Phys. Rev. Lett. **95**, 173901 (2005).
54. F. Mostafavi, M. Hong, R. B. Dawkins, *et al.*, "Multiphoton quantum Imaging using natural light," arXiv (2024).